

## Research Article

## SOX10-Internal Tandem Duplications and *PLAG1* or *HMGA2* Fusions Segregate Eccrine-Type and Apocrine-Type Cutaneous Mixed Tumors

Nicolas Macagno<sup>a,b,c,\*</sup>, Thibault Kervarrec<sup>a,d,e</sup>, Soumanth Thanguturi<sup>f</sup>, Pierre Sohier<sup>g</sup>, Daniel Pissaloux<sup>h,i</sup>, Lenaïg Mescam<sup>j</sup>, Marie-Laure Jullie<sup>k</sup>, Eric Frouin<sup>l</sup>, Amelie Osio<sup>m,n</sup>, Monique Faisant<sup>o</sup>, François Le Loarer<sup>p,q</sup>, Bernard Cribier<sup>r</sup>, Eduardo Calonje<sup>s</sup>, Evelyn Vanesa Erazo Luna<sup>s</sup>, Daniela Massi<sup>t</sup>, Keisuke Goto<sup>u</sup>, Haruto Nishida<sup>u</sup>, Sandrine Paindavoine<sup>h</sup>, Aurelie Houlier<sup>h</sup>, Juliet Tantot<sup>n</sup>, Nazim Benzerdjeb<sup>n</sup>, Franck Tirode<sup>h,i</sup>, Arnaud De la Fouchardière<sup>h,i</sup>, Maxime Battistella<sup>a,v</sup>

<sup>a</sup> CARADERM, French Network of Rare Skin Cancers, Lille, France; <sup>b</sup> Department of Pathology, APHM, Timone, Marseille, France; <sup>c</sup> Aix Marseille University, INSERM, MMG, Marseille, France; <sup>d</sup> Department of Pathology, Université de Tours, Centre Hospitalier Universitaire de Tours, Tours, France; <sup>e</sup> "Biologie des infections à polyomavirus" team, UMR INRA ISP 1282, Université de Tours, Tours, France; <sup>f</sup> Department of Pathology, « Institut d'histopathologie, Tours, France; <sup>g</sup> Department of Pathology, Hôpital Cochin, AP-HP, Centre-Université Paris Cité, Paris, France; <sup>h</sup> Department of Biopathology, Centre Léon Bérard, Lyon, France; <sup>i</sup> Université de Lyon, Université Claude Bernard Lyon 1, INSERM 1052, CNRS 5286, Centre Léon Bérard, Cancer Research Center of Lyon, Equipe Labellisée Ligue contre le Cancer, Lyon, France; <sup>j</sup> Department of Biopathology, Paoli-Calmettes Institute, Marseille, France; <sup>k</sup> Department of Pathology, University Hospital of Bordeaux, Bordeaux, France; <sup>l</sup> Department of Pathology, University Hospital of Poitiers, University of Poitiers, LITEC, Poitiers, France; <sup>m</sup> National Center of Dermatopathology, Paris-la Roquette, Ivry, France; <sup>n</sup> Department of Pathology, HCL Lyon-Sud Hospital, Lyon, France; <sup>o</sup> Cypath, Villeurbanne, France; <sup>p</sup> Department of Biopathology, Bergonié Institute, Bordeaux, France; <sup>q</sup> Bordeaux Institute of Oncology, BRIC U1312, INSERM, Université de Bordeaux, Institut Bergonié, Bordeaux, France; <sup>r</sup> Department of Dermatology, University of Strasbourg, Strasbourg, France; <sup>s</sup> Department of Dermatopathology, St John's Institute of Dermatology, Guy's and St Thomas' NHS trust, London, United Kingdom; <sup>t</sup> Section of Pathology, Department of Health Sciences, University of Florence, Florence, Italy; <sup>u</sup> Department of Diagnostic Pathology, Faculty of Medicine, Oita, Japan; <sup>v</sup> Department of Pathology, AP-HP Hospital Saint-Louis, INSERM U976, Université Paris Cité, Paris, France

## ARTICLE INFO

## Article history:

Received 31 May 2023

Revised 26 December 2023

Accepted 16 January 2024

Available online 23 January 2024

## Keywords:

chondroid syringoma

HMGA2

mixed tumor

myoepithelioma

PLAG1

SOX10

## ABSTRACT

Cutaneous mixed tumors exhibit a wide morphologic diversity and are currently classified into apocrine and eccrine types based on their morphologic differentiation. Some cases of apocrine-type cutaneous mixed tumors (ACMT), namely, hyaline cell-rich apocrine cutaneous mixed tumors (HCR-ACMT) show a prominent or exclusive plasmacytoid myoepithelial component. Although recurrent fusions of *PLAG1* have been observed in ACMT, the oncogenic driver of eccrine-type cutaneous mixed tumors (ECMT) is still unknown. The aim of the study was to provide a comprehensive morphologic, immunohistochemical, and molecular characterization of these tumors. Forty-one cases were included in this study: 28 cases of ACMT/HCR-ACMT and 13 cases of ECMT. After morphologic and immunohistochemical characterization, all specimens were analyzed by RNA sequencing. By immunohistochemistry, all cases showed expression of SOX10, but only ACMT/HCR-ACMT showed expression of *PLAG1* and *HMGA2*. RNA sequencing confirmed the presence of recurrent fusion of *PLAG1* or *HMGA2* in all cases of ACMT/HCR-ACMT, with a perfect correlation with *PLAG1*/*HMGA2* immunohistochemical status, and revealed internal tandem duplications of SOX10 (*SOX10-ITD*) in all cases of ECMT. Although *TRPS1::PLAG1* was the most frequent fusion, *HMGA2::WIF1* and *HMGA2::NFIB* were detected in ACMT cases. Clustering analysis based on gene expression profiling of 110 tumors, including numerous histotypes, showed that ECMT formed a distinct group compared with all other tumors. ACMT, HCR-ACMT, and salivary gland pleomorphic adenoma clustered together, whereas myoepithelioma with fusions of *EWSR1*, *FUS*, *PBX1*, *PBX3*, *POU5F1*, and *KLF17*

\* Corresponding author.

E-mail address: [nicolas.macagno@ap-hm.fr](mailto:nicolas.macagno@ap-hm.fr) (N. Macagno).

ELSEVIER

formed another cluster. Follow-up showed no evidence of disease in 23 cases across all 3 tumor types. In conclusion, our study demonstrated for the first time SOX10-ITD in ECMT and *HMG2* fusions in ACMT and further refined the prevalence of *PLAG1* fusions in ACMT. Clustering analyses revealed the transcriptomic distance between these different tumors, especially in the heterogeneous group of myoepitheliomas.

© 2024 United States & Canadian Academy of Pathology. Published by Elsevier Inc. All rights reserved.

## Introduction

Cutaneous adnexal tumors display wide morphologic diversity and have been traditionally classified based on their presumed line of differentiation based mainly on morphologic features. In recent years, the classification of adnexal neoplasms has been improved and become more accurate following the identification of specific molecular-driven abnormalities in certain fusion genes. These fusion genes are often shared with related tumors in other organs, particularly the salivary glands.

Cutaneous mixed tumors are morphologically divided into apocrine and eccrine types. Apocrine-type cutaneous mixed tumors (ACMT), formerly known as chondroid syringomas, are related to salivary pleomorphic adenomas and are the most common cutaneous tumors with myoepithelial differentiation.<sup>1</sup> ACMT is characterized by a dual population of epithelial and myoepithelial cells embedded in an abundant stroma with a wide range of matrix components that can be collagenous, myxoid, myxohyaline, chondroid, lipogenic, and even osteogenic. Although fusions of *PLAG1* and *HMG2* have been reported in the salivary glands with immunohistochemical overexpression of the corresponding proteins, only *PLAG1* fusions have been reported so far in cutaneous ACMT cases.<sup>2-4</sup>

Some cases of ACMT display a prominent or exclusive plasmacytoid myoepithelial component, namely, hyaline cell-rich apocrine cutaneous mixed tumors (HCR-ACMT).<sup>5-15</sup> Owing to this predominant myoepithelial differentiation with few or no ducts and fusion of *PLAG1*, these tumors have been labeled as *PLAG1*-rearranged cutaneous myoepithelioma<sup>3</sup> posing a problem of terminology between HCR-ACMT and soft tissue myoepithelioma/cutaneous syncytial myoepithelioma, which are tumors that also express myoepithelial markers but rather harbor fusions of *EWSR1* and *FUS*.<sup>16,17</sup>

The eccrine variant of cutaneous mixed tumor (ECMT), namely, chondroid syringoma with ductal features, is much rarer and so far, a defined genetic abnormality has not been described.<sup>4,18,19</sup> A rearrangement of *PLAG1* gene has not been detected in this neoplasm.<sup>4</sup> Similar to its apocrine counterpart, ECMT also presents with a prominent stroma but lacks the dual population observed in the former.<sup>18</sup> Furthermore, the stroma is less variable than an apocrine variant, being myxoid in most cases.

In this context, the present study aimed to provide a detailed morphologic, immunohistochemical, and molecular characterization of cutaneous mixed tumors with comprehensive transcriptomic analyses.

## Materials and Methods

### Histologic Examination

Cases were retrieved from the authors' consultation files and reviewed in the French network for rare skin cancers (CARADERM, [www.caraderm.org](http://www.caraderm.org)). Four cases of acral cutaneous mixed tumors

have been published in a recent work by our team: 3 cases with molecular data were included in this study, details of which are available in [Supplementary Table S1](#).<sup>20</sup> Archived slides with hematoxylin, phloxin, and saffron staining and immunohistochemistry (IHC) were reviewed for noteworthy details. Follow-up was collected from the referring physician or the patient's medical records. The study was performed in accordance with the Declaration of Helsinki and was approved by the research ethics committee of the Centre Léon Bérard (CLB, reference: L17-63).

Diagnoses were based on the histopathologic criteria of the 5th edition of the WHO classification of cutaneous tumors<sup>21</sup> but also incorporating the latest molecular data.<sup>22-26</sup>

Tumors were defined as apocrine-type cutaneous mixed tumors (ACMT), formerly known as chondroid syringoma, if all 3 epithelial, myoepithelial, and mesenchymal components were readily identifiable. Morphologic apocrine differentiation such as decapitation secretion and follicular differentiation were evaluated. A subset of ACMT composed almost entirely of myoepithelial plasmacytoid cells has been identified and described under the term "hyaline cell-rich chondroid syringoma" or hyaline cell-rich apocrine-type cutaneous mixed tumors (HCR-ACMT). These tumors are composed of plasmacytoid cells with hyaline cytoplasm embedded in a variable amount of stroma. In the 5th edition of the WHO Classification of Tumors of the Skin, it is stated that a small subset of the so-called "myoepitheliomas" shows "PLAG1 rearrangements and lacks ductal differentiation" and are characterized by "lobulated, trabecular, or nested architecture with variably epithelioid, spindled, plasmacytoid, or clear cells within a myxoid or hyalinized stroma," which overlaps morphologically with HCR-ACMT. In the current study, tumors with *PLAG1* fusion and predominance of a plasmacytoid myoepithelial component were not considered true myoepithelioma but rather a hyaline cell-rich-ACMT (HCR-ACMT) and analyzed near the ACMT group.

Of note, HCR-ACMT cases were not selected for inclusion in the study based on morphologic features without considering the molecular characteristics but rather included from a larger group characterized by a molecular criterion based on the presence of fusion of *PLAG1*. This group included cases that have been previously published by our group, focusing on acral site tumors, detailed in [Supplementary Table S1](#).<sup>20</sup>

Finally, tumors composed of simple monolayered tubules associated with mesenchymal stroma were classified as eccrine-type cutaneous mixed tumors (ECMT), formerly known as chondroid syringoma with ductal features.

In addition to the morphologic histotype, other features evaluated included the presence of follicular cysts, decapitation secretion, plasmacytoid cytology, clear cell changes, formation of hyaline rosettes, peripheral lymphoid rim, pleomorphism (high-grade atypia), necrosis, and mitotic count (per 2 mm<sup>2</sup>) and the average proportion of epithelial, myoepithelial, and mesenchymal components were semiquantitatively evaluated. Stroma was considered present if it occupied more than 5% of the tumor surface area and included myxoid, collagenous, fibrohyaline, lipogenic, chondroid, amyloid, and osteogenic.

## Immunohistochemistry

Paraffin block sections were stained for SOX10, P63, EMA, CEA, keratin 8/18, keratin 7, PLAG1, and HMGA2, using the Ventana Benchmark Ultra automated immunostainer (Ventana Medical Systems and detected using the UltraView Universal DAB Detection Kit [Ventana]). Details of the clones are available in the [Supplementary Table S1](#).

## Anchored Multiplex PCR RNA Sequencing on Formalin-Fixed Paraffin-Embedded Samples

The rearrangements of *PLAG1*, *HMGA2*, *FUS*, and *EWSR1* were investigated by next-generation sequencing. The library was prepared using a custom FusionPlex Comprehensive kit (ArcherDx) to generate target-enriched libraries and sequenced on a MiSeq System (Illumina). The resulting data were analyzed using Archer Analysis Suite v6.03.2. AMP (Anchored Multiplex PCR) technology. This custom panel is derived from the comprehensive thyroid and lung and includes several genes useful in the diagnosis of adnexal neoplasms, such as *AKT1*, *ALK*, *EWSR1*, *MAML2*, *MYB*, *NTRK1*, *NTRK2*, *NTRK3*, *NUTM1*, *PLAG1*, *RET*, *ROS1*, and *YAP1*, as well as *AXL*, *BRAF*, *CCND1*, *CCND3*, *CIITA*, *DUSP22*, *FGFR1*, *FGFR2*, *FGFR3*, *MALT1*, *NRG1*, *PDCD1LG2*, *PPARG*, *RAF1*, *SS18*, *THADA*, and *TP63*. Notably, *HMGA2*, *SOX10*, and *NFIB* were not analyzed by this custom panel, but this approach allows the detection of a fusion transcript if only one of the 5' or 3' partners is detectable in the panel.

## Whole-Exome Capture RNA Sequencing on Formalin-Fixed Paraffin-Embedded Samples

Exome-based RNA capture sequencing was performed on formalin-fixed paraffin-embedded samples, and the data were further analyzed to detect fusion genes and small nucleotide variations and to compare expression profiles with more than 6000 other samples from the Centre Léon Bérard (CLB) molecular database using clustering methods. The molecular basis of the technique, the technical protocol, and the bioinformatics algorithms used have been described previously.<sup>27</sup> In addition to the detection of gene fusions using different algorithms, the Arriba command-line tool was also used to detect other structural rearrangements with potential clinical relevance, such as internal tandem duplications. Internal tandem duplications (ITD) were validated in all cases by local alignment to a region of 400 nucleotides around the ITD. Ward's unsupervised clustering and Uniform Manifold Approximation and Projection (UMAP) were performed in the R (v4.2. 2) environment using the cluster and UMAP packages, respectively, on all cases of ECMT and 12 cases of ACMT/HCR-ACMT from our cohort for comparison with the transcriptomic data of 85 other tumors, including other cases of ACMT, pleomorphic adenoma of the salivary glands, cutaneous hidradenoma with *CRTC1::MAML2* or *CRTC3::MAML2* fusion, cutaneous poroma and porocarcinoma with *YAP1::MAML2* or *YAP1::NUTM1* fusion, cutaneous trichogerminoma with *GRHL1*, *GHRL2*, and *GHRL3* fusion, cutaneous basal cell carcinoma with *PTCH1* or *SMO* mutations, cutaneous syncytial and soft tissue myoepithelioma with *EWSR1* and *PBX1/PBX3* or *POU5F1* fusion, and myoepithelioma with *KLF17* fusion. Other cases included Merkel cell carcinoma and proliferating pilar tumor. Details of the molecular findings, including fusions and mutations are provided for all cases in [Supplementary Table S2](#).

**Table 1**

Clinicopathologic characteristics of the cohort (n = 41)

	ACMT (n = 15)	HCR-ACMT (n = 13)	ECMT (n = 13)
Age, y (range)	67 (26-81)	61 (19-82)	62 (38-81)
Median size, mm (range)	14 (6-37)	11 (7-35)	12 (3-70)
Location (%)			
Acral sites	6 (46)	7 (53)	0 (0)
Head	7 (50)	3 (21)	4 (31)
Limbs	0 (0)	3 (60)	4 (31)
Trunk	2 (33)	0 (0)	4 (31)
Vulva	0 (0)	0 (0)	1 (7)
Formation of ducts			
Absent	0 (0)	6 (46)	0 (0)
Rare <sup>a</sup>	0 (0)	7 (54)	0 (0)
Obvious	15 (100)	0 (0)	13 (100)

ACMT, apocrine-type cutaneous mixed tumor; ECMT, eccrine-type cutaneous mixed tumor; HCR-ACMT, hyaline cell-rich apocrine-type cutaneous mixed tumor.

<sup>a</sup> Requires high-magnification or immunohistochemistry.

## Results

### Clinical and Histopathologic Characteristics of the Cohort

Forty-one cutaneous tumors consisting of 28 cases of ACMT/HCR-ACMT including 7 cases exclusively myoepithelial and 13 cases of ECMT were included in the study. The clinicopathologic features of the cases are listed in [Table 1](#).

Briefly, 21 patients were male and 20 were female, the sex ratio M:F was 1.15:1 for ACMT/HCR-ACMT, and 1:2 for ECMT. The median age at diagnosis was 59 years (range: 19-82 years).

The tumor locations included the acral sites (n = 13/41), trunk (n = 6/41), head (n = 14/41), arm (n = 3/41), groin (n = 3/41), buttocks (n = 1/41), and vulva (n = 1/41). Location was not specified in 1 case. No cases of ECMT occurred on acral sites. The median tumor size was 14 mm (range: 6-37 mm) for ACMT/HCR-ACMT and 12 mm (range: 3-8 mm) for ECMT.

The overall morphologic features of ACMT/HCR-ACMT and ECMT are shown in [Figure 1](#), the details of the 2 *HMGA2*-rearranged ACMT cases are shown in [Figure 2](#), and the morphologic details of cases of ECMT are available in [Figure 3](#).

ACMT (n = 15) and HCR-ACMT (n = 13) differed by the presence of readily identifiable ducts lined by 2 cell layers in the former and the prominence of the plasmacytoid myoepithelial cells in the latter. In all cases of ACMT, the myoepithelial component consisted of a population of eosinophilic myoepithelial cells, with plasmacytoid appearance, surrounding ducts, forming solid aggregates, or consisting of isolated cells surrounded by stroma. When present, the epithelial component was organized as branching ducts and tubules, with the formation of cystic structures in 13% of cases. Decapitation secretion (77% of cases) and follicular differentiation (4% of cases) were also noted. The ducts were barely identifiable and required immunohistochemistry in 6 cases (21%). One case of ACMT showed a peripheral lymphoid rim. None of the ACMT cases showed pseudorosette, clear cells, mitotic activity, pleomorphism, or necrosis, except for 2 cases: 1 located on the scalp and measuring 25 mm, which showed occasional multinucleated cells and random bizarre nuclei (ancient atypia) but no diffuse pleomorphism, necrosis, or mitotic activity ([Fig. 2B](#)), with no recurrence or metastatic spread for this case at 397 days of follow-up; and 1 located on the facial area which consisted a well-circumscribed

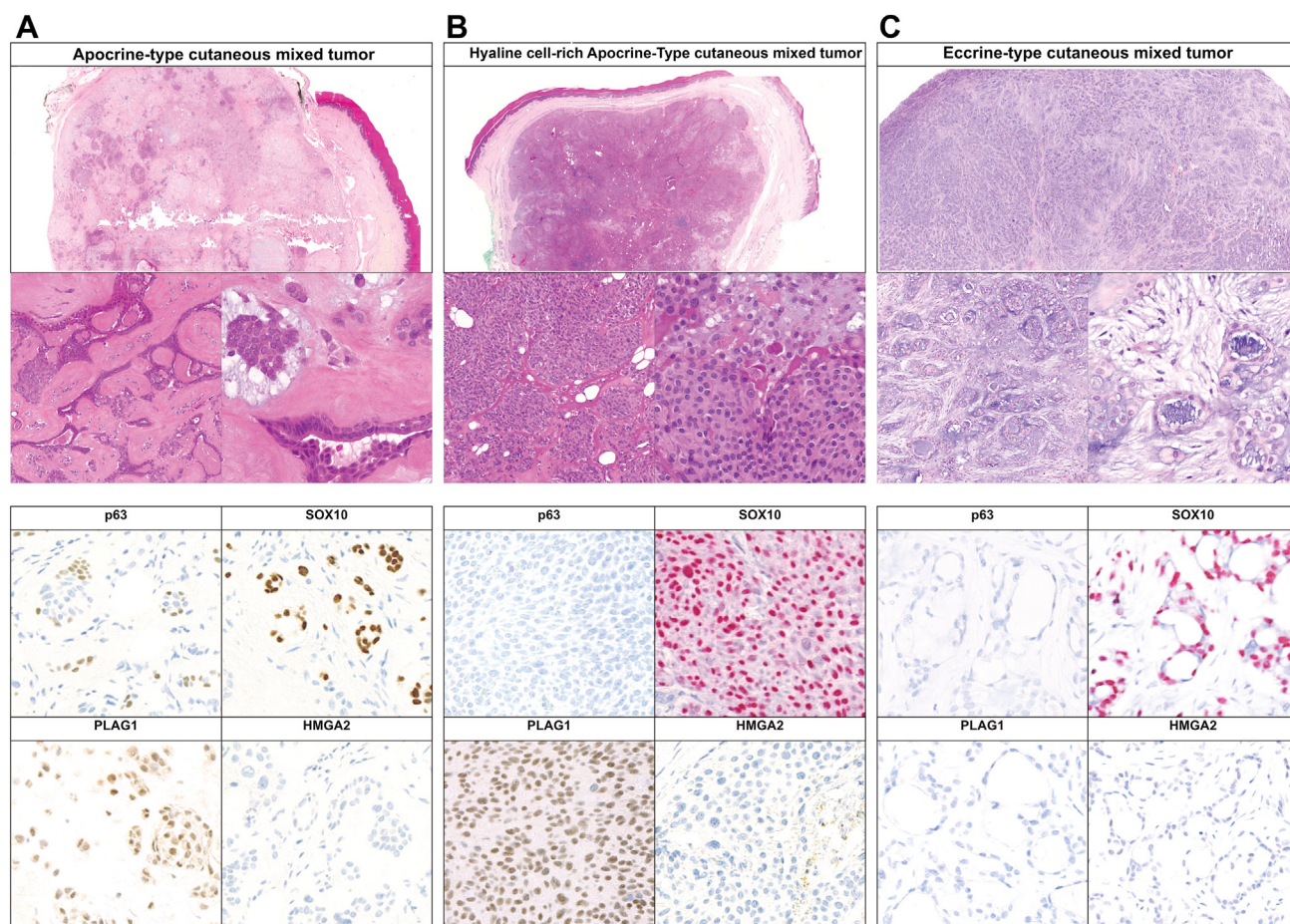


**Figure 1.**

Morphologic and immunohistochemical features of cutaneous mixed tumors. (A) Apocrine cutaneous mixed tumor (ACMT) with *TRPS1::PLAG1* fusion showing a dual population of cells, with apocrine secretion, embedded in a fibrohyaline mesenchymal stroma, with immunohistochemical nuclear expression of p63, SOX10, and PLAG1 but negativity for HMGA2. (B) Hyaline cell-rich apocrine cutaneous Mixed Tumor (HCR-ACMT) with *TRPS1::PLAG1* fusion showing aggregates of myoepithelial cells, often with plasmacytoid cytology, often absent expression of p63, diffuse expression of SOX10 and PLAG1, and lack of expression of HMGA2. (C) Eccrine cutaneous mixed tumor (ECMT) with *SOX10-ITD* is composed of a bland and monotonous proliferation of eosinophilic cells, often arranged in round tubes or isolated cells, embedded in an abundant fibromyxoid stroma, with a diffuse expression of SOX10, no expression of P63, PLAG1, and HMGA2.

lesion of 9 mm, with 6 mitoses per mm<sup>2</sup> and focal necrosis but no pleomorphism – this case also showed the highest Ki67 index of the cohort (20%).

The cases of exclusively myoepithelial HCR-ACMT (n = 7) lacked ductal structure by morphologic examination and immunohistochemistry and were defined by an exclusive composition of hyaline plasmacytoid myoepithelial cells forming solid aggregates or isolated cells surrounded by stroma. No cases showed pseudorosette, clear cells, or peripheral lymphoid rim, mitotic activity, pleomorphism, or necrosis.

Morphologic details of cases of ECMT are available in [Figure 3](#) and [Supplementary Figure S1](#). The 13 cases of ECMT lacked the dual population of epithelial–myoepithelial cells and were composed of somewhat monotonous, medium-sized cells with pink, often hyaline cytoplasm, and oval or round vesicular nuclei with an inconspicuous nucleolus, organized in round tubular structures, nests, cords, and individual units. Arrangement of tumor cells in hyaline rosettes was present in 2 cases (15%). All cases of ECMT showed individual cells with plasmacytoid appearance within the stroma. Decapitation secretion and follicular cysts were absent in all cases of ECMT. One case showed clear cell change, and 6 cases displayed a peripheral lymphoid rim.

The mean tumor surface represented by the mesenchymal component was 66% for ECMT, 48% for ACMT/HCR-ACMT, and 20% for exclusively myoepithelial HCR-ACMT. All cases of ECMT showed a prominent myxoid matrix.

All cases evaluated ([Table 2](#)) showed diffuse SOX10 positivity by immunohistochemistry. Keratin expression was available for 35/41 cases. In ECMT, CK8/18 was diffusely positive in 5 cases and focally positive in 1 case. In ACMT/HCR-ACMT, CK8/18 was diffusely positive in 15 cases and focally in 9 cases. The cytokeratin 7 expression overlapped with CK8/18 expression in 14 cases but was positive in a case of ACMT negative for CK8/18. S100 expression was present in all 17 cases evaluated, including 13/13 cases of ACMT/HCR-ACMT and 4/4 cases of ECMT. Nuclear expression of p63 was diffusely positive in 8/12 cases of ACMT/HCR-ACMT and focally positive in 1/9 cases of ECMT. The Ki67 proliferation index, available for 4 cases of ACMT/HCR-ACMT and 3 cases of ECMT never exceeded 5% except for 1 case of ACMT with mitotic activity in which it was 20%.

Nuclear expression of PLAG1 and HMGA2 was absent in all ECMT cases but was observed in 2 cases of ACMT/HCR-ACMT, which showed diffuse HMGA2 nuclear staining, whereas 16/18 cases of ACMT/HCR-ACMT (88%) showed

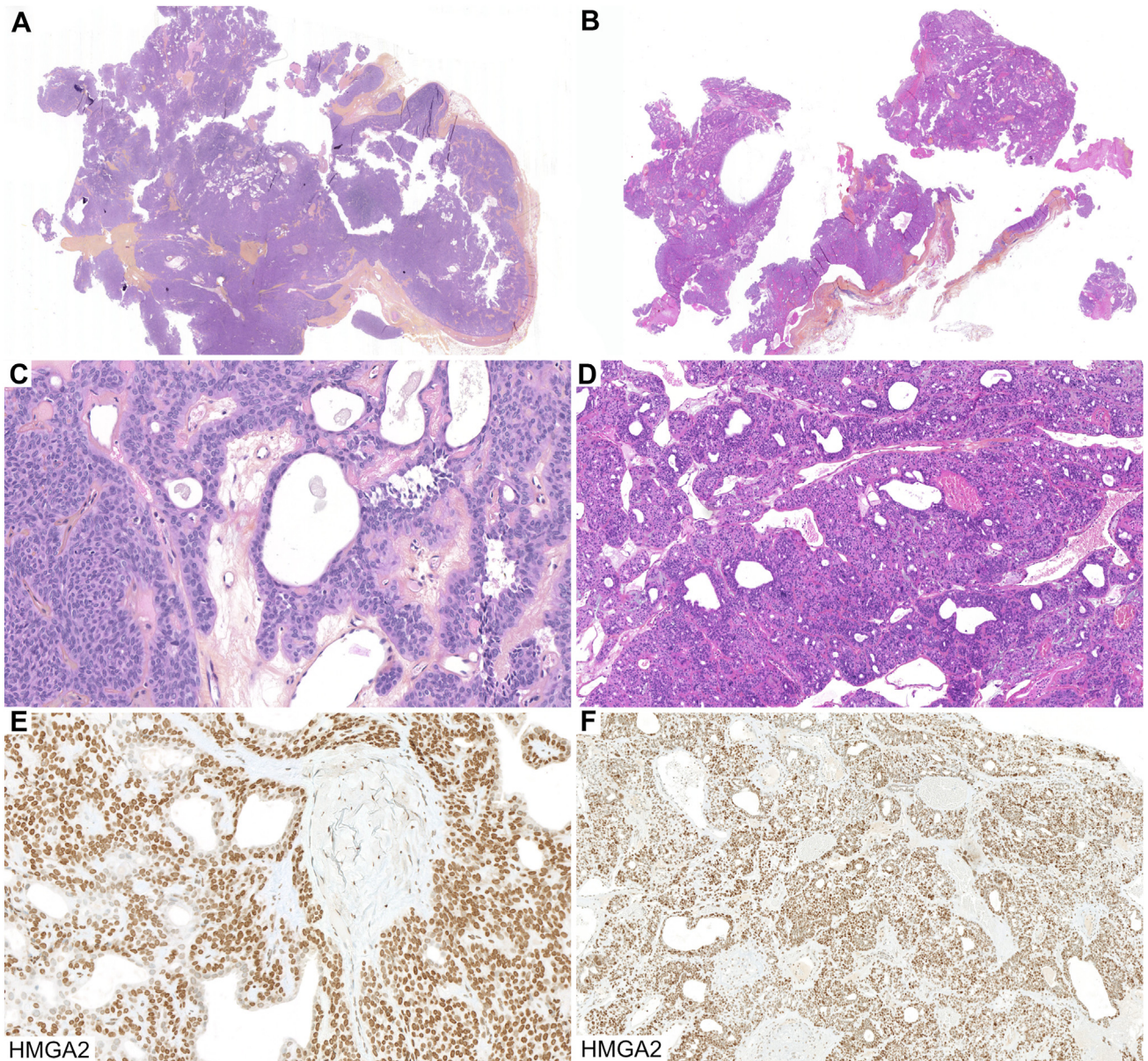


**Figure 2.**

Morphologic and immunohistochemical features of apocrine cutaneous mixed tumors (ACMT) with *HMGA2* rearrangement (A, C, E). (A) A 32-mm tumor of the trunk wall with *HMGA2::WIF1* fusion and the morphologic features of ACMT, including a dual population of cells, luminal apocrine decapitation, and frequent cysts. The stroma is fibrohyaline (A, C). There is diffuse and intense nuclear expression of *HMGA2* (E). (B, D, F) A 25-mm tumor of the scalp with *HMGA2::NFIB* fusion with the morphologic features of ACMT, with a dual population of cells, frequent cysts, and random bizarre nuclei (ancient atypia), but no diffuse pleomorphism, necrosis, or mitotic activity (B, D). The stroma is scarce, often loose, and myxoid. There is diffuse and intense nuclear expression of *HMGA2* (F).

diffuse nuclear *PLAG1* expression. *HMGA2* and *PLAG1* expression was mutually exclusive and always correlated with the type of gene fusion detected by molecular biology. Morphologic and immunohistochemical details of the 2 *HMGA2*-rearranged ACMT/HCR-ACMT cases are shown in Figure 2.

Taken together, these findings further support that ACMT/HCR-ACMT shows a variable proportion of myoepithelial, epithelial, and stromal components and expression of *PLAG1* or *HMGA2* even in cases with an exclusive myoepithelial component, whereas ECMT have distinctive morphologic and immunohistochemical features.

#### *Fusions of PLAG1 and HMGA2 Are Restricted to the ACMT/HCR-ACMT Group*

Because recurrent *PLAG1*, *HMGA2*, and *EWSR1* rearrangements have been reported in neoplasms with myoepithelial differentiation of the skin and other organs, we investigated our cohort by anchored multiplex PCR RNA sequencing (n = 16) and exome-based RNA capture sequencing on FFPE samples (n = 25). No case was analyzed by either of the methods. The molecular findings of the cohort are listed in Table 3. Molecular insights from each RNA sequencing approach are available in Supplementary Table S1.

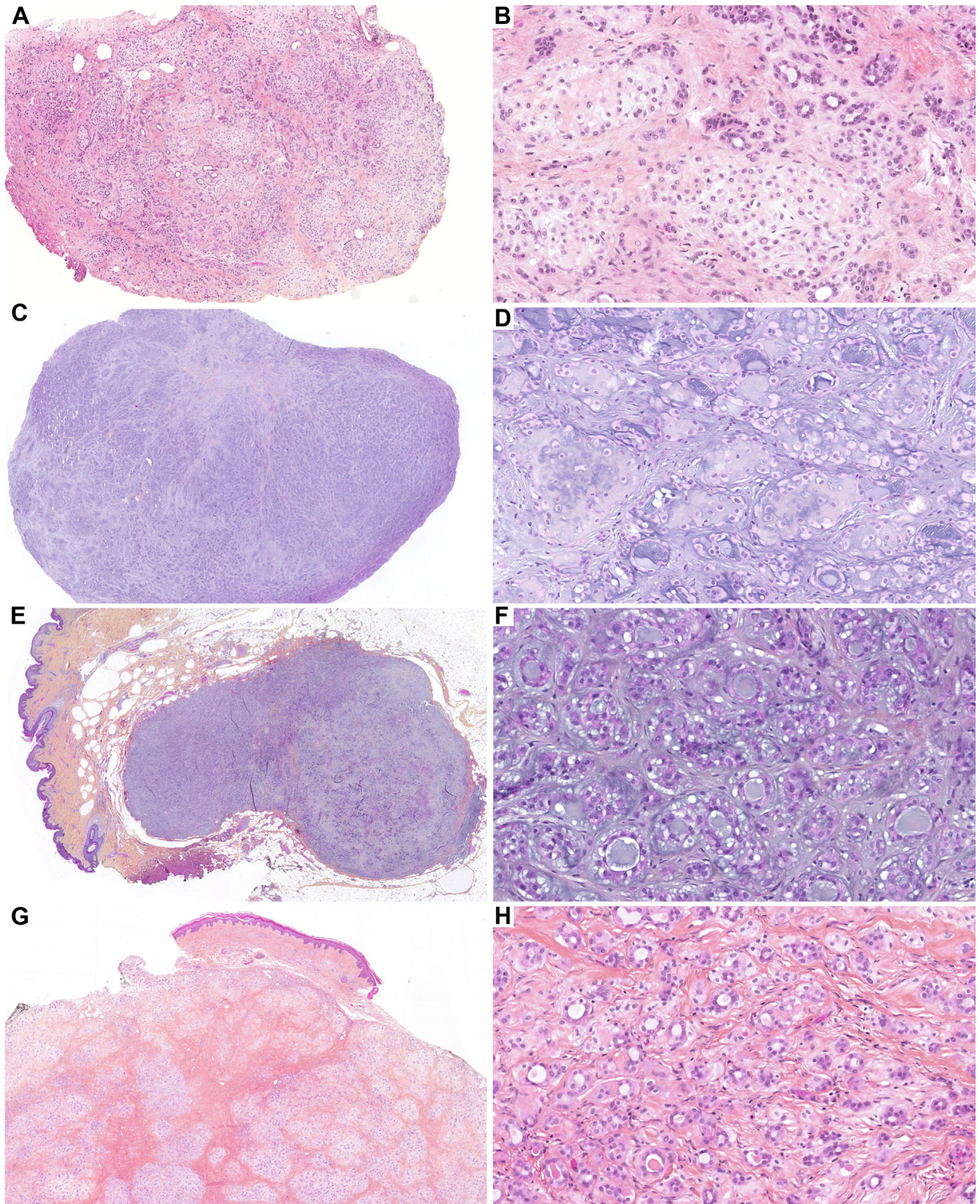


**Figure 3.**

(A) Morphologic features of eccrine cutaneous mixed tumors (ECMT) with internal tandem duplication of SOX10 (ITD-SOX10): an example of ECMT showing a dermal nodular silhouette with alternating loose myxoid nodules and fibrous stroma. (B) Higher magnification shows simple monolayered rounded tubules and isolated cells embedded in myxohyaline stroma. Some cells are organized around hyaline rosettes. (C) A second example of ECMT shows a nodular silhouette with abundant deep basophilic myxoid matrix and fibrohyaline rosettes. (D) Isolated round cells embedded in these hyaline islands give a chondroid appearance. (E, F) Another dermo-hypodermal example of ECMT is with a peripheral lymphoid rim (E), in which the cells are arranged in cords and round structures (F). (G, H) This last example shows a more abundant fibrous stroma (G) and occasional clear cell cytology (H).

**Table 2**

Immunohistochemical profiling of the tumors (n = 41)

	ACMT (%)	HCR-ACMT (%)	ECMT (%)
SOX10	13/13 (100)	12/12 (100)	11/11 (100)
Diffuse	13/13 (100)	12/12 (100)	11/11 (100)
PLAG1	8/10 (80)	8/8 (100)	0/11 (0)
Diffuse	8/10 (80)	8/8 (100)	0/11 (0)
HMGA2	2/10 (20)	0/8 (0)	0/5 (0)
Diffuse	2/10 (20)	0/8 (0)	0/5 (0)
p63	11/12 (92)	8/12 (66)	1/11 (9)
Diffuse	5/12 (42)	2/12 (16)	0/11 (0)
Focal	6/12 (50)	6/12 (50)	1/11 (9)
ACE	4/10 (40)	6/12 (50)	4/11 (36)
Diffuse	0/10 (0)	2/12 (16)	0/11 (0)
Focal	4/10 (40)	4/12 (33)	4/11 (36)
CK8/18 or CK7	12/12 (100)	10/12 (83)	6/11 (54)
Diffuse	9/12 (75)	3/12 (25)	5/11 (45)
Focal	3/12 (23)	7/12 (58)	1/11 (9)

ACE, angiotensin-converting enzyme; ACMT, apocrine-type cutaneous mixed tumor; ECMT, eccrine-type cutaneous mixed tumor; HCR-ACMT, hyaline cell-rich apocrine-type cutaneous mixed tumor; HMGA2, High Mobility Group AT-Hook 2; PLAG1, pleomorphic adenoma gene 1; SOX10, SRY-Box Transcription Factor 10.

Consistent with the immunohistochemical findings, the molecular data revealed recurrent gene fusions in all 28 ACMT/HCR-ACMT cases studied, involving the genes *PLAG1* (n = 26/28, 93%) and *HMGA2* (n = 2/28, 7%). In the 13 ECMT cases, no fusion of *PLAG1* and *HMGA2* was detected. In *PLAG1*-rearranged cases, the most common fusion was *TRPS1::PLAG1* (n = 21/28, 78%), whereas *CTNNB1::PLAG1*, *LIFR::PLAG1*, *GEM::PLAG1*, *RNU6-895P::PLAG1*, and *NCALD::PLAG1* fusions were detected in 1 case each (3.5%). In *HMGA2*-rearranged ACMT/HCR-ACMT cases, *HMGA2::WIF1* and *HMGA2::NFIB* were detected in 1 case each (3.5%).

The expression of *PLAG1* and *HMGA2* protein correlated with the molecular status in all cases, with *PLAG1* gene fusions (*TRPS1::PLAG1*, *RNU6-895P::PLAG1*, and *NCALD::PLAG1* fusions) being detected in all 16 cases with positive *PLAG1* immunostaining. The *HMGA2::WIF1* and *HMGA2::NFIB* fusions were detected in the 2 ACMT cases that lacked *PLAG1* expression but showed diffuse nuclear *HMGA2* expression.

**Table 3**

Proportion and types of molecular alterations detected in the different tumor subtypes studied (n = 41)

	ACMT (n=15)	HCR-ACMT (n = 13)	ECMT (n = 13)
PLAG1 fusion	13/15 (87)	13/13 (100)	0/13 (0)
<i>TRPS1::PLAG1</i>	12/15 (80)	9/13 (69)	0/13 (0)
<i>RNU6-895P::PLAG1</i>	0/15 (0)	1/13 (8)	0/13 (0)
<i>NCALD::PLAG1</i>	0/15 (0)	1/13 (8)	0/13 (0)
<i>LIFR::PLAG1</i>	0/15 (0)	1/13 (8)	0/13 (0)
<i>GEM::PLAG1</i>	0/15 (0)	1/13 (8)	0/13 (0)
<i>CTNNB1::PLAG1</i>	1/15 (7)	0/13 (0)	0/13 (0)
HMGA2 fusion	2/15 (13)	0/13 (0)	0/13 (0)
<i>HMGA2::NFIB</i>	1/15 (7)	0/13 (0)	0/13 (0)
<i>HMGA2::WIF1</i>	1/15 (7)	0/13 (0)	0/13 (0)
SOX10 rearrangement	0/15 (0)	0/13 (0)	13/13 (100)
SOX10-ITD	0/7 (0)	0/5 (0)	13/13 (100)

ACMT, apocrine-type cutaneous mixed tumor; ECMT, eccrine-type cutaneous mixed tumor; HCR-ACMT, hyaline cell-rich apocrine-type cutaneous mixed tumor.

### Internal Tandem Duplications of *SOX10* (*SOX10-ITD*) Are Restricted to the ECMT Group

Although no recurrent gene fusion was detected in ECMT, analysis of our cases revealed recurrent internal tandem duplications within the *SOX10* gene in all ECMT cases (13/13, 100%), whereas *SOX10-ITD* was absent in the other neoplasms analyzed by the same method (n = 12). The duplication was confined to exon 4, based on *SOX10* transcript ENST00000396884 (NM\_006941.4). Notably, this duplication involved sequences located in the transactivation domain<sup>28</sup> and consistently included the residues 288-302 including an EØ[D/E]QYØ motif (residues 296-301, Fig. 4) recently shown to be critical for *SOX10* function.<sup>29</sup>

Therefore, our results suggest that *SOX10-ITD* is a recurrent molecular finding of ECMT compared with the ACMT/HCR-ACMT group, which shows *PLAG1* and *HMGA2* fusion, similar to pleomorphic adenoma, its salivary counterpart.

### Clustering Analyses

Clustering analyses using gene expression profiling were performed on 110 tumors, including the cases of ECMT (n = 13), ACMT (n = 7), and HCR-ACMT (n = 5) of the present cohort with other cases of the following neoplasms: ACMT (n = 3), salivary gland pleomorphic adenoma (n = 17), poroma (n = 3), porocarcinoma (n = 5), cutaneous hidradenoma (n = 5), trichogerminoma (n = 13); basal cell carcinoma, Merkel cell carcinoma (n = 8), proliferating pilar tumor (n = 6), and soft tissue or cutaneous syncytial myoepithelioma (n = 19). The UMAP is shown in Figure 4 and the molecular details of each group are available in Supplementary Table S2.

All ECMTs showed high transcriptomic proximity and formed a distinct group, with a large transcriptomic distance to other neoplasms in general, including the group of ACMT/HCR-ACMT. Clustering analyses further confirmed similar gene expression profiles and great proximity between cases diagnosed morphologically as ACMT and HCR-ACMT but also with pleomorphic adenoma of the salivary gland. These findings suggest a transcriptional proximity between these neoplasms, regardless of the tumor site.

In addition, comparative analyses with 19 cases of myoepithelioma with *EWSR1::PBX1* (n = 4), *EWSR1::PBX3* (n = 8), *EWSR1::POU5F1* (n = 3), *FUS::KLF17* (n = 2), and *EPS15::KLF17* (n = 2) fusions showed divergent transcriptomic profiles compared with the ACMT, HCR-ACMT, salivary gland pleomorphic adenoma and ECMT groups.

### Follow-Up Data

Follow-up data are summarized in Table 4. Most patients were lost to follow-up due to a diagnosis of "benign tumor" but data were available for 23 patients, including 6 patients with ACMT, 8 patients with HCR-ACMT, and 8 patients with ECMT. Median follow-up was 489 days (range: 55-7533 days). All patients were alive with no evidence of disease. The only case with increased mitotic activity in our cohort showed no evidence of recurrence at 397 days of follow-up. Two patients had positive margins and one of these patients benefited from a second surgery to achieve a clear margin, both are still free of recurrence at 2371 and 321 days of follow-up, respectively.

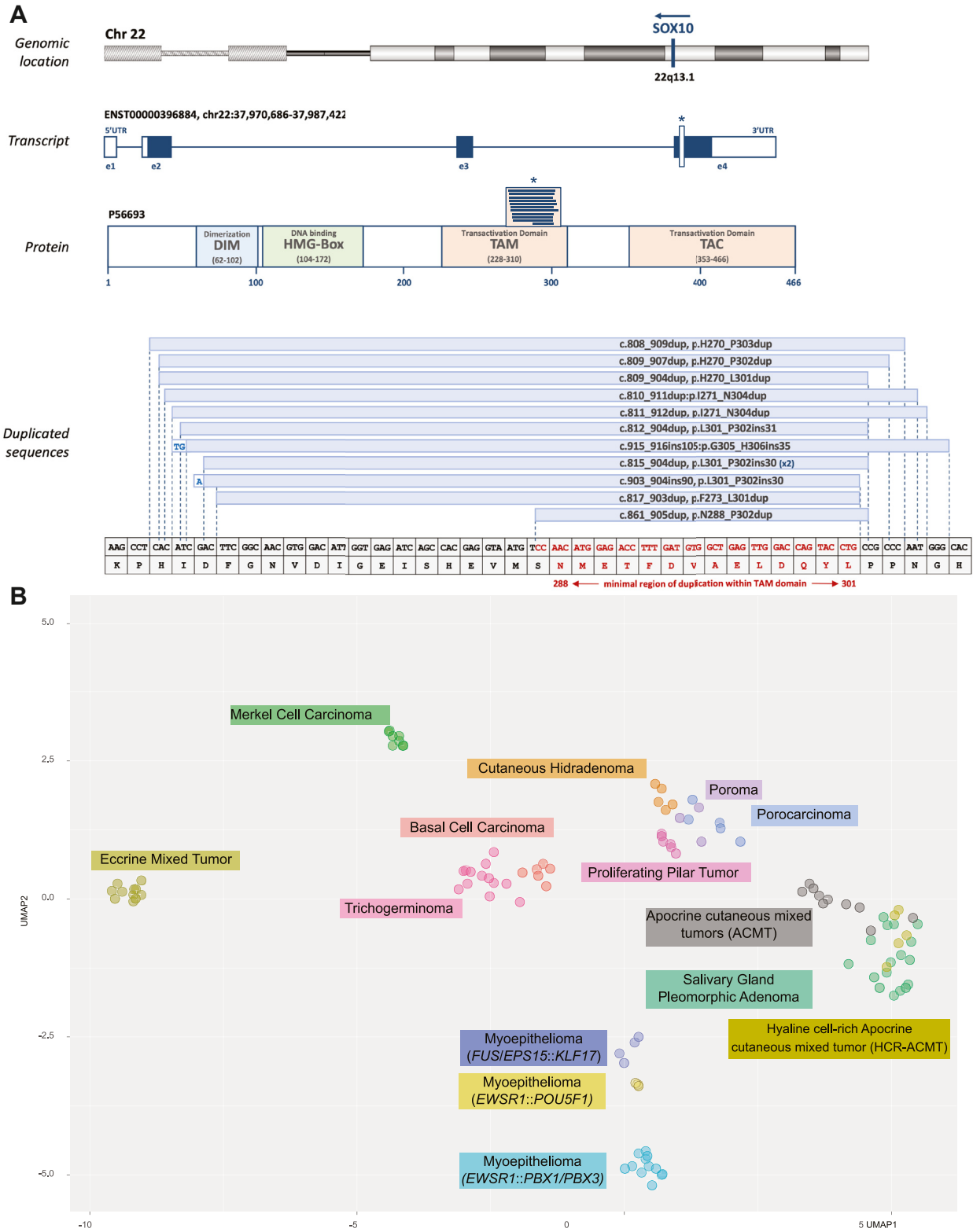


**Figure 4.**

(A) Details of the internal duplication of SOX10 in all cases of eccrine cutaneous mixed tumor (ECMT): the duplication involved sequences located in the exon 4, which contains the transactivation domain and consistently included the residues 288-302 including an E0[D/E]QY0 motif (residues 296-301). An asterisk (\*) indicates the position of the duplicated sequences within the transactivation domain. (B) UMAP projection of the transcriptome of 110 cases: apocrine cutaneous mixed tumor (ACMT), Hyaline cell-rich apocrine cutaneous mixed tumor (HCR-ACMT), eccrine cutaneous mixed tumor (ECMT), basal cell carcinoma, cutaneous hidradenoma, poroma, porocarcinoma, myoepithelioma, proliferating pilar tumor, trichogerminoma, and Merkel cell carcinoma. The cases of ECMT form a robust cluster with transcriptomic distance to the other tumors, strongly suggesting a distinct neoplasm. Notably, cases of pleomorphic adenoma of the salivary gland and ACMT/HCR-ACMT show overlapping transcriptomic profiles and are distinct from myoepithelioma with *EWSR1::PBX1*, *EWSR1::PBX3*, *EWSR1::POU5F1*, *FUS::KLF17*, and *EPS15::KLF17* fusion.

**Table 4**

Follow-up data of the cohort (n = 23)

Diagnosis	Age (y)	Location	Size (mm)	Molecular alteration	Mitosis per mm <sup>2</sup>	Pleomorphism	Follow-up (days)	Status
ACMT	55	Face	12	TRPS1::PLAG1	0	0	55	NED
ACMT	77	Foot	37	TRPS1::PLAG1	0	0	227	NED
ACMT	71	Scalp	25	HMGA2:NFB	0	0	397	NED
ACMT	73	Face	6	TRPS1::PLAG1	0	0	338	NED
ACMT	75	Face	10	TRPS1::PLAG1	0	0	496	NED
ACMT	26	Face	10	TRPS1::PLAG1	0	0	712	NED
ACMT	40	Face	10	TRPS1::PLAG1	0	0	72	NED
ECMT	53	Trunk	4	ITD-SOX10	0	0	90	NED
ECMT	74	Face	12	ITD-SOX10	0	0	109	NED
ECMT	48	Trunk	12	ITD-SOX10	0	0	120	NED
ECMT	64	Groin	12	ITD-SOX10	0	0	259	NED
ECMT	43	Vulva	10	ITD-SOX10	0	0	976	NED
ECMT	81	Scalp	4	ITD-SOX10	0	0	7533	NED
ECMT	62	Trunk wall	15	ITD-SOX10	0	0	1086	NED
ECMT	71	Trunk wall	3	ITD-SOX10	0	0	1116	NED
HCR-ACMT	76	Face	9	GEM::PLAG1	6	0	308	NED
HCR-ACMT	19	Foot	11	RNU6-895P::PLAG1	0	0	345	NED
HCR-ACMT	44	Face	9	LIFR::PLAG1	0	0	489	NED
HCR-ACMT	65	Face	11	TRPS1::PLAG1	0	0	577	NED
HCR-ACMT	71	Buttock	35	NCALD::PLAG1	0	0	884	NED
HCR-ACMT	56	Foot	23	TRPS1::PLAG1	0	0	945	NED
HCR-ACMT	62	Foot	16	TRPS1::PLAG1	0	0	1001	NED
HCR-ACMT	36	Arm	7	TRPS1::PLAG1	0	0	2013	NED

ACMT, apocrine-type cutaneous mixed tumor; ECMT, eccrine-type cutaneous mixed tumor; HCR-ACMT, hyaline cell–rich apocrine-type cutaneous mixed tumor; NED, no evidence of disease.

## Discussion

In the present study, we have demonstrated that cutaneous mixed tumor of the eccrine type shows recurrent internal tandem duplication of the *SOX10* gene (*SOX10*-ITD). We have also confirmed the presence of recurrent fusion of *PLAG1* or *HMGA2* in ACMT and HCR-ACMT and further highlighted their morphologic, immunohistochemical, and molecular features.

The eccrine variant of cutaneous mixed tumors was first described by Headington in 1961.<sup>19</sup> In a large series of 50 cases, Kazakov et al<sup>18</sup> further delineated the clinicopathologic features of ECMT which usually presents as a small solitary nodule with predilection for the head and neck of adults and histologically consists of a well-defined nodule located in the dermis with occasional extension into the subcutaneous tissue. In their report, the epithelial component of ECMT was described as forming small round tubules lined by a single layer of cuboidal cells with bland cytology lacking decapitation secretion and embedded in an abundant stroma. Prominent cribriform areas, clear cell changes, rosette formation, prominent bony metaplasia, and physaliphorous-like cells represent unusual morphologic features.<sup>18</sup> Reflecting the lack of a dual cell population, immunohistochemical studies showed a lack of expression of p63, whereas EMA, CK7, and S100 proteins were variably expressed.

Herein, we have confirmed the lack of p63 expression in most cases of ECMT tested in our cohort and have shown that although *SOX10* is always diffusely expressed in ECMT, the same pattern is seen in ACMT/HCR-ACMT. Russel-Goldman et al<sup>4</sup> reported *PLAG1* immunohistochemical expression in 16 ACMT and 9 ECMT and found that *PLAG1* positivity was restricted to ACMT suggesting an alternative oncogenic driver for this tumor. Consistent with this observation, in our study, nuclear expression of *PLAG1* and *HMGA2* was restricted to cases of ACMT/HCR-ACMT.

Although a feature of ACMT, particularly in the prominent myoepithelial component of HCR-ACMT, the plasmacytoid

appearance due to eccentrically located nuclei has been reported in some cases of ECMT.<sup>18</sup> Indeed, hyaline scattered cells have been reported in approximately 80% of ECMT cases. As pointed out by Kazakov et al,<sup>18</sup> "the nuclei were located at the periphery of the cells, resulting in a resemblance to the so-called "hyaline" (plasmacytoid) cells seen in the apocrine-mixed tumor, but smaller" in ECMT. However, unlike its apocrine counterpart, ECMT does not show evidence of apocrine secretion or differentiation along other lines of the folliculosebaceous–apocrine unit, and all reported cases of ECMT showed the formation of tubules. As pointed out by Kazakov et al,<sup>18</sup> the presence of pseudorosettes is specific but rare. Pseudorosettes were specific but only present in 15% of ECMT cases in our cohort. Further studies are needed to evaluate the exact morphologic differences between HCR-ACMT and ECMT. Finally, our results for *HMGA2* and *PLAG1* expression in ACMT, HCR-ACMT, and ECMT provide diagnostic value in this context.

Molecular analysis of our series of ECMT by whole-exome RNA sequencing revealed recurrent *SOX10*-ITD in all cases. *SOX10* (*SRY*-related HMG-box 10) encodes a transcription factor involved in the regulation of embryonic development and cell fate determination and is critical for the maintenance and differentiation of multipotent neural crest cells, the peripheral nervous system, and the sweat glands.<sup>30</sup>

Overexpression and mutations in *SOX10* have been found in several tumor types, highlighting its role in oncogenesis, notably in melanoma where *SOX10* serves as a lineage survival oncogene, promoting proliferation and survival.<sup>31</sup> Accordingly, loss-of-function mutations in *SOX10*, often removing all or part of the transactivation domain,<sup>32</sup> are observed in the Waardenburg–Shah syndrome,<sup>30</sup> an autosomal dominant condition characterized by the association of sensorineural deafness and pigmentary defects. After homodimerization and binding to the promoter or enhancer regions, *SOX10* transactivates its target genes through interaction with its transactivation (residues 228–310) and C terminal domains (353–466). In particular, the highly conserved EØ[D/E]QYØ

motif (residues 296–301) is critical for the transactivation function.<sup>29</sup> Our data show that the ITD partially involves sequences in this motif, which is crucial for the activity of protein and could change the regulation patterns and lead to aberrant SOX10 function, uncontrolled proliferation, or prevent differentiation in ECMT. Ideally, experimental validation will be required to confirm the oncogenic nature of this ITD, including overexpression of ITD-SOX10 in relevant cell lines and testing for increased proliferation and oncogenic properties, as well as assessing how it affects the downstream targets of SOX10. Experimental validation and further analysis would be essential steps to understand the full significance of this new molecular finding. ITD are tandem duplications within coding exons – in our cohort it was exon 4 of *SOX10*. ITDs have been previously described in the *BCOR* gene in sarcomas<sup>33</sup> and central nervous system tumors<sup>34</sup> and in *FLT3* in acute myeloid leukemia.<sup>35</sup> Detection of ITDs requires appropriate tools such as digital droplet PCR or RNA sequencing data with appropriate algorithms.<sup>36</sup> Most of the molecular data in our study is derived from exome-based RNA sequencing, and caveats associated with calling variants based solely on RNA sequencing may affect the reliability of calling ITDs, including limitations due to the level of expression, as low levels of RNA cannot be detected, and limitations due to the nature of the ITD, which, similar to a truncating mutation, may be associated with high mRNA decay. Although very unlikely, our approach could not exclude a germline pathogenic variant, as no comparison to germline DNA was performed.

Following a previously reported method, we performed Ward's unsupervised clustering and Uniform Manifold Approximation and Projection (UMAP) within the R (v4.2.2) environment, using cluster and UMAP packages, respectively, on ECMT/ACMT/HCR-ACMT and other tumors that revealed high transcriptomic proximity between ECMT cases, forming a robust and highly isolated cluster, suggesting that they may not represent a true variant of a mixed tumor but rather a distinct entity with a single type of cells showing myoepithelial differentiation, which is the expected definition of a myoepithelioma, ie, a neoplasm composed exclusively of myoepithelial cells. However, our data further suggested high proximity between ACMT, HCR-ACMT, and pleomorphic adenoma of the salivary glands, which are composed of several types of cells in most cases, thus meeting the definition of a mixed tumor.

Due to morphologic and immunohistochemical evidence of myoepithelial differentiation, it has been suggested that mixed tumors be classified within the spectrum of myoepithelial tumors, namely, myoepitheliomas. Whether mixed tumors and myoepitheliomas are part of the same spectrum or represent distinct tumor entities remains controversial<sup>37,38</sup> because of the prominent and sometimes exclusive myoepithelial component in cases of *PLAG1*-rearranged tumors, which have been termed myoepithelioma with or without ducts.<sup>1,39</sup> In our cohort, 13 cases associated with *PLAG1* fusion showed a prominent myoepithelial differentiation, meeting the definition of HCR-ACMT, including 7 cases with an exclusive myoepithelial component, the so-called “*PLAG1*-rearranged myoepithelioma.” Interestingly, the publication by Ferreiro et al<sup>12</sup> that first coined the hyaline cell-rich terminology already reported a case of HCR-ACMT lacking ducts. Other types of myoepitheliomas usually lack ductal formation and have a different molecular signature, lacking *PLAG1* and *HMGA2* fusion and instead having rearrangements of TLS family genes such as *EWSR1* and *FUS*, with multiple partners including *ZNF444*, *PBX1*, *PBX3*, *KLF17*, and *POU5F1*.<sup>16,40</sup>

In this context, the current WHO classification defines myoepithelioma as a neoplasm “composed exclusively of myoepithelial

cells” with *PLAG1* and *EWSR1* rearrangement cited as defining genetic alteration.<sup>41</sup> In contrast, the mixed tumor is defined as “a benign sweat gland neoplasm composed of epithelial, myoepithelial, and mesenchymal elements”<sup>2</sup> with myoepithelioma cited in this chapter as “a related entity distinguished by the lack of ductal structures”.<sup>2</sup> In fact, it is well established in the literature that there is a gray area between these 2 groups of tumor entities, with several authors claiming that they belong to the same spectrum<sup>1</sup> and using the term mixed tumor/myoepithelioma.<sup>37</sup> In particular, Kazakov et al<sup>39</sup> mentioned “cases of cutaneous tumors that have the morphology of a typical myoepithelioma revealing only exceptional ductal structures.” Similarly, Antonescu et al<sup>3</sup> reported a series of skin and soft tissue myoepithelioma with ductal differentiation and *PLAG1* rearrangement.<sup>42</sup> In the series of cutaneous myoepitheliomas published by Mehta et al,<sup>39</sup> “rare duct differentiations were frequently noted” as well as frequent *PLAG1* expression suggesting *PLAG1* rearrangement.

Consistent with these findings, in the present study we confirmed at the morphologic, immunohistochemical, and molecular levels that ACMT and HCR-ACMT including purely myoepithelial cases were closely related tumor entities with variable levels of myoepithelial differentiation that shared the same oncogenic drivers, namely, *PLAG1* and *HMGA2* fusion akin to their salivary counterparts.

Previous publications, including the recent report by Mehta et al,<sup>39</sup> have observed prominent myoepithelial differentiation in *PLAG1*-rearranged acral cutaneous mixed tumors.<sup>3,20,39</sup> This prominent myoepithelial differentiation was indeed present in acral cases in our cohort, but only in slightly more than half of the acral cases, including 5 cases with a hyaline cell-rich morphology with a prominent plasmacytoid myoepithelial component and 2 cases with an exclusively myoepithelial plasmacytoid component, with the remaining cases showing a more common chondroid syringoma morphology because ducts were readily identifiable. Other sites with a prominent or exclusive myoepithelial component included the face (3 cases), arm (1 case), buttock (1 case), and elbow (1 case).

Furthermore, our clustering analyses of myoepitheliomas with *PBX1*, *PBX3*, *POU5F1*, and *KLF17* showed transcriptomic proximity to each other, but not to the group of *PLAG1*/*HMGA2* rearranged ACMT/cutaneous myoepitheliomas and pleomorphic adenomas of the salivary glands. In the soft tissues, several molecular subtypes of myoepithelioma have been described that share specific morphologic features: myoepitheliomas with *POU5F1* fusions often have worrisome features, occur at a younger age, and are composed of lobules or nests of clear cells and those with *PBX1*/*PBX3* fusions show a sclerotic spindle cell morphology, whereas *PBX3* fusions have been described in the cutaneous syncytial variant, including lipogenic cases.<sup>25–27</sup> Myoepitheliomas with *KLF17* fusions have a chordoma-like morphology that can be confused with ECMT if the stroma is myxoid.<sup>28</sup> In the skin, *EWSR1*-rearranged cutaneous myoepitheliomas have been reported in the literature as syncytial myoepitheliomas and are characterized by frequent syncytial morphology, expression of S100 protein, and absence of keratin expression.<sup>5</sup> In the skin, syncytial myoepithelioma likely represents a distinct tumor entity that is much rarer than HCR-ACMT. In our cohort, plasmacytoid morphology was present in all cases studied, a common finding in ACMT, HCR-ACMT, and ECMT. Our study lacks data to conclude the specificity of this morphologic finding, suggesting that further investigations are needed, focusing on the correlation between morphology and the type of fusions of myoepithelial tumors. Finally, clustering analyses showed that eccrine mixed tumors had a very distinct transcriptomic profile compared with other tumors,

suggesting that they may not even represent a true variant of a mixed tumor but rather a distinct entity. In this context, we believe that the general term "myoepithelioma" is too confusing as it encompasses too many different neoplasms with distinct molecular findings, clinical presentation, morphology, and perhaps prognosis. In this regard, we believe that "PLAG1-rearranged cutaneous myoepithelioma" is not the best term to refer to HCR-ACMT with prominent and/or exclusive myoepithelial components.

Further studies are needed to investigate their molecular proximity to molecularly characterized myoepitheliomas with *FUS* or *EWSR* fusion. Transcriptomic or methylation studies may help assess molecular proximity in these entities.

Given their molecular heterogeneity, the prognosis of myoepitheliomas as a whole is notoriously difficult to predict. However, the limited follow-up data of our cohort showed that cases diagnosed as ACMT/HCR-ACMT and ECMT showed indolent behavior, including one case with mitotic activity and cases with positive surgical margins. More data are needed to further confirm these findings, based on bona fide cases confirmed by a specific immunohistochemical or molecular hallmark.

Another important finding concerned 2 of our cases of ACMT that showed fusion of *HMGA2*, a feature not previously reported in the skin. Given the small number of cases, it is difficult to conclude specific morphologic features from our cohort. However, in the salivary glands, *HMGA2*-rearranged pleomorphic adenoma cases are characterized by a distinct trabecular (canalicular adenoma-like) morphology.<sup>43</sup> One case with *HMGA2::NFIB* showed occasional multinucleated cells without mitotic activity or necrosis, which is described as a possible finding in pleomorphic adenoma, called bizarre tumor cells (ancient atypia) in the WHO classification of salivary gland tumors.

In conclusion, the present study identified recurrent *SOX10*-ITD in ECMT, a tumor with a very distinct and unique transcriptomic profile. Our data further confirmed that cutaneous ACMT including the HCR-ACMT variant with prominent or exclusive myoepithelial component belongs to a spectrum of neoplasms defined by *PLAG1* and *HMGA2* fusions, with close transcriptomic profiles to their salivary analog, namely, pleomorphic adenoma, but distant from myoepithelial tumors with fusion involving the *EWSR1*, *FUS*, *PBX1*, *PBX3*, *POU5F1*, and *KLF17* genes.

#### Author Contributions

N.M., T.K., S.T., P.S., L.M., M.L.J., E.F., A.O., M.F., F.L.L., B.C., E.C., D.M., K.G., H.N., N.B., and J.T. provided cases. N.M., T.K., P.S., and M.B. reviewed cases. F.T., D.P., A.H., S.P. performed molecular and statistical analyses. N.M., T.K., P.S., and M.B. wrote the manuscript. E.C., D.M., B.C., and A.D.L.F. reviewed and edited the manuscript.

#### Data Availability

Raw data were generated at the Centre Léon Bérard, Lyon, France (F.T.). Derived data supporting the findings of this study are available in [Supplementary Table S2](#) and from the corresponding author (N.M.) upon request.

#### Funding

This research received no specific grant from any funding agency in the public, commercial, or not-for-profit sectors.

#### Declaration of Competing Interest

The authors have no conflicts of interest to disclose.

#### Ethics Approval and Consent to Participate

The study was performed in accordance with the Declaration of Helsinki and was approved by the research ethics committee of the Centre Léon Bérard (CLB, reference: L17-63). A waiver of consent was granted for this work.

#### Supplementary Material

The online version contains supplementary material available at <https://doi.org/10.1016/j.modpat.2024.100430>

#### References

- Mentzel T, Requena L, Kaddu S, Soares de Aleida LM, Sanguenza OP, Kutzner H. Cutaneous myoepithelial neoplasms: clinicopathologic and immunohistochemical study of 20 cases suggesting a continuous spectrum ranging from benign mixed tumor of the skin to cutaneous myoepithelioma and myoepithelial carcinoma. *J Cutan Pathol*. 2003;30:294–302. <https://doi.org/10.1034/j.1600-0560.2003.00063.x>
- Sanguenza OP, Cassarino DS, Glusac EJ, et al. *Mixed tumour. WHO Classification of Skin Tumour*. 4th edition volume. Lyon: IARC; 2018.
- Antonescu CR, Zhang L, Shao SY, et al. Frequent *PLAG1* gene rearrangements in skin and soft tissue myoepithelioma with ductal differentiation. *Genes Chromosomes Cancer*. 2013;52:675–682. <https://doi.org/10.1002/gcc.22063>
- Russell-Goldman E, Dubuc A, Hanna J. Differential expression of *PLAG1* in apocrine and eccrine cutaneous mixed tumors: evidence for distinct molecular pathogenesis. *Am J Dermatopathol*. 2020;42:251–257. <https://doi.org/10.1097/DAD.0000000000001393>
- Nakayama H, Kishi A, Kajihara H. Hyaline cell-rich chondroid syringoma: epithelial nature of the hyaline cells. *Jpn J Clin Oncol*. 1996;26:237–242. <https://doi.org/10.1093/oxfordjournals.jjco.a023221>
- Kazakov DV, Bisceglia M, Spagnolo DV, et al. Apocrine mixed tumors of the skin with architectural and/or cytologic atypia: a retrospective clinicopathologic study of 18 cases. *Am J Surg Pathol*. 2007;31:1094–1102. <https://doi.org/10.1097/PAS.0b013e3180309e4d>
- Kazakov DV, Kacerovska D, Skalova A, et al. Cutaneous apocrine mixed tumor with intravascular tumor deposits: a diagnostic pitfall. *Am J Dermatopathol*. 2011;33:775–779. <https://doi.org/10.1097/DAD.0b013e31820b7b9c>
- Ito FA, Jorge J, Vargas PA, Lopes MA. Histopathological findings of pleomorphic adenomas of the salivary glands. *Med Oral Patol Oral Cirurgia Bucal*. 2009;14:E57–E61. PMID: 19179950.
- Mukit M, Ortanca I, Krassilnik N, Dadireddy K. Chondroid syringoma of the thenar eminence in a US Veterans Administration (VA) patient. *Eplasty*. 2021;21:ic4. PMID: 34025902.
- Ohata C. Hyaline cell-rich apocrine mixed tumor with cytologic atypia. *Dermatopathol Basel Switz*. 2018;5:108–112. <https://doi.org/10.1159/000492668>
- Reis-Filho JS, Silva P, Milanezi F, Lopes JM. Hyaline cell-rich chondroid syringoma: case report and review of the literature. *Pathol Res Pract*. 2002;198:755–764. <https://doi.org/10.1078/0344-0338-00332>
- Ferreiro JA, Nascimento AG. Hyaline-cell rich chondroid syringoma. A tumor mimicking malignancy. *Am J Surg Pathol*. 1995;19:912–917. <https://doi.org/10.1097/00000478-199508000-00006>
- Masamatti SS, Vijaya C, Narasimha A. A rare case of hyaline cell-rich atypical chondroid syringoma with divergent differentiation. *Indian J Pathol Microbiol*. 2018;61:428–430. [https://doi.org/10.4103/IJPM.IJPM\\_101\\_17](https://doi.org/10.4103/IJPM.IJPM_101_17)
- Ramaswamy AS, Yenni VV, Wilfred C, Manjunatha HK, Shilpa K. Hyaline cell-rich chondroid syringoma of the finger. *Indian J Dermatol*. 2011;56:217–219. <https://doi.org/10.4103/0019-5154.80424>
- Sharma S, Chatterjee D, Kanwar A. Hyaline cell-rich chondroid syringoma: a potential pitfall on cytology. *Diagn Cytopathol*. 2023;51:E351–E354. <https://doi.org/10.1002/dc.25223>
- Jo VY, Antonescu CR, Dickson BC, et al. Cutaneous syncytial myoepithelioma is characterized by recurrent *EWSR1*-*PBX3* fusions. *Am J Surg Pathol*. 2019;43:1349–1354. <https://doi.org/10.1097/PAS.0000000000001286>
- Jo VY, Antonescu CR, Zhang L, Dal Cin P, Hornick JL, Fletcher CDM. Cutaneous syncytial myoepithelioma: clinicopathologic characterization in a series of 38 cases. *Am J Surg Pathol*. 2013;37:710–718. <https://doi.org/10.1097/PAS.0b013e3182772bba>

18. Kazakov DV, Kacerovska D, Hantschke M, et al. Cutaneous mixed tumor, eccrine variant: a clinicopathologic and immunohistochemical study of 50 cases, with emphasis on unusual histopathologic features. *Am J Dermatopathol*. 2011;33:557–568. <https://doi.org/10.1097/DAD.0b013e318206c1a3>
19. Headington JT. Mixed tumors of skin: eccrine and apocrine types. *Arch Dermatol*. 1961;84:989–996. <https://doi.org/10.1001/archderm.1961.01580180105016>
20. Kervarrec T, Tallet A, Macagno N, et al. Sweat gland tumors arising on acral sites: a molecular survey. *Am J Surg Pathol*. 2023;47:1096–1107. <https://doi.org/10.1097/PAS.0000000000002098>
21. Elder DE, Massi D, Scolyer RA, Willemze R. *WHO Classification of Skin Tumours*. International Agency for Research on Cancer; 2018.
22. Hile G, Harms PW. Update on molecular genetic alterations of cutaneous adnexal neoplasms. *Surg Pathol Clin*. 2021;14:251–272. <https://doi.org/10.1016/j.path.2021.03.004>
23. Plotzke JM, Adams DJ, Harms PW. Molecular pathology of skin adnexal tumours. *Histopathology*. 2022;80:166–183. <https://doi.org/10.1111/his.14441>
24. Macagno N, Sohier P, Kervarrec T, et al. Recent advances on immunohistochemistry and molecular biology for the diagnosis of adnexal sweat gland tumors. *Cancers*. 2022;14:476. <https://doi.org/10.3390/cancers14030476>
25. Kervarrec T, Sohier P, Pissaloux D, et al. Genetics of adnexal tumors: an update. *Ann Dermatol Venerol*. 2023;150:202–207. <https://doi.org/10.1016/j.annder.2023.03.003>
26. Kervarrec T, Pissaloux D, Tirode F, et al. Gene fusions in poroma, porocarcinoma and related adnexal skin tumours: an update. *Histopathology*. 2024;84(2):266–278. <https://doi.org/10.1111/his.1502327>
27. Macagno N, Pissaloux D, de la Fouchardière A. Wholistic approach – transcriptomic analysis and beyond using archival material for molecular diagnosis. *Genes Chromosomes Cancer*. 2022;61(6):382–393. <https://doi.org/10.1002/gcc.23026>
28. Pusch C, Hustert E, Pfeifer D, et al. The SOX10/Sox10 gene from human and mouse: sequence, expression, and transactivation by the encoded HMG domain transcription factor. *Hum Genet*. 1998;103:115–123. <https://doi.org/10.1007/s004390050793>
29. Haseeb A, Lefebvre V. The SOXE transcription factors-SOX8, SOX9 and SOX10-share a bi-partite transactivation mechanism. *Nucleic Acids Res*. 2019;47:6917–6931. <https://doi.org/10.1093/nar/gkz523>
30. Pingault V, Zerad L, Bertani-Torres W, Bondurand N. SOX10: 20 years of phenotypic plurality and current understanding of its developmental function. *J Med Genet*. 2022;59:105–114. <https://doi.org/10.1136/jmedgenet-2021-108105>
31. Liu J, Fukunaga-Kalabis M, Li L, Herlyn M. Developmental pathways activated in melanocytes and melanoma. *Arch Biochem Biophys*. 2014;563:13–21. <https://doi.org/10.1016/j.abb.2014.07.023>
32. Bondurand N, Dastot-Le Moal F, Stanchina L, et al. Deletions at the SOX10 gene locus cause Waardenburg syndrome types 2 and 4. *Am J Hum Genet*. 2007;81:1169–1185. <https://doi.org/10.1086/522090>
33. Kao Y-C, Owosho AA, Sung Y-S, et al. BCOR-CCNB3 fusion positive sarcomas: a clinicopathologic and molecular analysis of 36 cases with comparison to morphologic spectrum and clinical behavior of other round cell sarcomas. *Am J Surg Pathol*. 2018;42:604–615. <https://doi.org/10.1097/PAS.0000000000000965>
34. Ferris SP, Velazquez Vega J, Aboian M, et al. High-grade neuroepithelial tumor with BCOR exon 15 internal tandem duplication—a comprehensive clinical, radiographic, pathologic, and genomic analysis. *Brain Pathol Zurich Switz*. 2020;30:46–62. <https://doi.org/10.1111/bpa.12747>
35. Lagunas-Rangel FA, Chávez-Valencia V. FLT3-ITD and its current role in acute myeloid leukaemia. *Med Oncol Northwood Lond Engl*. 2017;34:114. <https://doi.org/10.1007/s12032-017-0970-x>
36. Baretts D, Appay R, Heinisch M, et al. Specific and sensitive diagnosis of BCOR-ITD in various cancers by digital PCR. *Front Oncol*. 2021;11:645512. <https://doi.org/10.3389/fonc.2021.645512>
37. Bahrami A, Dalton JD, Krane JF, Fletcher CDM. A subset of cutaneous and soft tissue mixed tumors are genetically linked to their salivary gland counterpart. *Genes Chromosomes Cancer*. 2012;51:140–148. <https://doi.org/10.1002/gcc.20938>
38. Mehta A, Davey J, Gharpuray-Pandit D, et al. Cutaneous myoepithelial neoplasms on acral sites show distinctive and reproducible histopathologic and immunohistochemical features. *Am J Surg Pathol*. 2022;46(9):1241–1249. <https://doi.org/10.1097/PAS.0000000000001896>
39. Kazakov DV, Michal M, Kacerovska D, McKee PH. Lesion with myoepithelial differentiation. In: *Cutaneous Adnexal Tumors*. Wolters Kluwer Health/Lippincott Williams and Wilkins; 2012.
40. Flucke U, Palmedo G, Blankenhorn N, Slootweg PJ, Kutzner H, Mentzel T. EWSR1 gene rearrangement occurs in a subset of cutaneous myoepithelial tumors: a study of 18 cases. *Mod Pathol Off JUS Can Acad Pathol Inc*. 2011;24:1444–1450. <https://doi.org/10.1038/modpathol.2011.108>
41. Hornick JL, Fisher C, LeBoit PE. Myoepithelioma *WHO Classification of Skin Tumours*. Volume 11. Lyon: IARC. 4th edition.
42. Jo VY, Fletcher CDM. Myoepithelial neoplasms of soft tissue: an updated review of the clinicopathologic, immunophenotypic, and genetic features. *Head Neck Pathol*. 2015;9:32–38. <https://doi.org/10.1007/s12105-015-0618-0>
43. Agaimy A, Ihrler S, Baněčková M, et al. HMGA2-WIF1 rearrangements characterize a distinctive subset of salivary pleomorphic adenomas with prominent trabecular (canalicular adenoma-like) morphology. *Am J Surg Pathol*. 2022;46:190–199. <https://doi.org/10.1097/PAS.0000000000001783>